GPR39 Knockout Worsens Microcirculatory Response to Experimental Stroke in a Sex-Dependent Manner

Yifan Xu
Oregon Health & Science University
Wenri Zhang
Oregon Health & Science University
Elyse Allen
Oregon Health & Science University
Lev Fedorov
Oregon Health & Science University
Anthony Barnes
Oregon Health & Science University
Zu Yuan Qian
Oregon Health & Science University
Thierno Bah
Oregon Health & Science University
Yuandong Li
University of Washington School of Medicine
Ruikang Wang
University of Washington School of Medicine
Robert Shangraw
Oregon Health & Science University
Nabil Alkayed (alkayedn@ohsu.edu)
Oregon Health & Science University

Research Article

Keywords: G protein-coupled receptor 39, capillary flux, pericytes, no-reflow, OMAG, sex difference

Posted Date: July 13th, 2022

DOI: https://doi.org/10.21203/rs.3.rs-1839951/v1

Abstract

Background and Purpose

No current treatments target microvascular reperfusion after stroke, which can contribute to poor outcomes even after successful clot retrieval. The G protein-coupled receptor GPR39 is expressed in brain peri-capillary pericytes, and has been implicated in microvascular regulation, but its role in stroke is unknown. We tested the hypothesis that GPR39 plays a protective role after stroke, in part due to preservation of microvascular perfusion. We generated GPR39 knockout (KO) mice and tested whether GPR39 gene deletion worsens capillary blood flow and exacerbates brain injury and functional deficit after focal cerebral ischemia.

Methods

Stroke was induced in male and female GPR39 KO and WT littermates by 60-minute middle cerebral artery occlusion (MCAO). Microvascular perfusion was assessed via capillary red blood cell (RBC) flux in deep cortical layers in vivo using optical microangiography (OMAG). Brain injury was assessed by measuring infarct size by 2,3,5-triphenyltetrazolium chloride staining at 24 hours or brain atrophy at 3 weeks after ischemia. Pole and cylinder behavior tests were conducted to assess neurological function deficit at 1 and 3 weeks post-stroke.

Results

Male but not female GPR39 KO mice exhibited larger infarcts and lower capillary RBC flux than WT controls after stroke. Male GPR39 KO mice also exhibited worse neurologic deficit at 1 week post-stroke, though functional deficit disappeared in both groups by 3 weeks.

Conclusions

GPR39 deletion worsens brain injury, microvascular perfusion, and neurological function after experimental stroke. Results indicate that GPR39 plays a sex-dependent role in re-establishing microvascular flow and limiting ischemic brain damage after stroke.

Introduction

Stroke is the second leading cause of death globally, with ischemic stroke accounting for 87% of all strokes. Globally, strokes account for 34% of global total healthcare expenditure. While t-PA clot lysis and endovascular clot retrieval have revolutionized stroke treatment, only a small percentage of patients qualify for these procedures and have access to centers that perform them. Patients who undergo clot retrieval have variable functional recovery, with a third to half of patients having poor outcome despite

undergoing endovascular therapy. Success at large vessel recanalization may not be accompanied by the expected restoration of downstream microvascular reperfusion. This “no-reflow” phenomenon across microvascular capillary beds may be secondary to perivascular edema, pericapillary cells compressing the delicate vessels, continued occlusion by small irretrievable clots, or inadequate blood flow or blood pressure to reopen small vessels.[5] Neurons have high metabolic demand, utilizing near 1:1 capillary:neuron neurovascular coupling to maintain optimal oxygenation and waste removal. Persistent capillary dysfunction would consequently lead to neural starvation and death in the affected watershed. Factors contributing to poor outcome after clot retrieval include vascular comorbidities such as atherosclerosis or diabetes mellitus.[6]

GPR39 is a member of the ghrelin family of G protein-coupled receptors. It plays a homeostatic role in vascular regulation, neuronal excitability and inflammation. Expressed in human brain peri-capillary pericytes and microglia, GPR39 has been implicated in moderating vascular inflammation and preventing excitotoxicity.[7,] GPR39 has been implicated in several neurological disorders, including cerebral small vessel disease-related dementia.[8] The endogenous ligand for GPR39 is uncertain, but it has been shown to sense the balance between vasodilator and vasoconstrictor eicosanoids, which contribute to the dynamic regulation of capillary blood flow.[,] GPR39 can also be activated by high concentrations of zinc which are known to occur during cerebral ischemia and may contribute to neurotoxicity.[7,,] These converging lines of reasoning suggest that GPR39 may play a role in the response to acute ischemic stroke. In this study, we used CRISPR/Cas9-mediated GPR39 gene deletion to generate GRP39 KO mice. We next used these mice to assess effect of GPR39 loss on post-ischemic microvascular flow, tissue injury and functional deficits in the setting of focal, transient cerebral ischemia. Our findings indicate that GPR39 KO mice exhibit persistently impaired microvascular blood flow after reperfusion despite restored macrocirculation, leading to exacerbated ischemic brain injury and concomitantly worse neurological deficits.

Methods

Data are available from the corresponding author on reasonable request. This article adheres to the American Heart Association Journals Implementation of Transparency and Openness Promotion Guidelines, including the ARRIVE 2.0 guidelines for reporting animal research. Detailed methods are available in the Supplemental Material.

Generation of GPR39 knockout mice

Mice with targeted GPR39 deletion were generated via CRISPR targeting technology.[,] Multiple guide RNAs (gRNAs) were designed that flank GPR39 exon 1 and each screened for DNA cleavage efficiency in murine Neuro 2A (N2A) cells (Invitrogen). A mixture containing 30 ng/μl of the two optimal gRNAs (Supplemental Table S1) and 100 ng/μl of the Cas9 mRNA (Trilink Biotech) was prepared, injected into zygotes of C57BL/6NJ mice (Jackson Laboratory, Stock #005304). The zygotes were transferred into

oviducts of pseudopregnant CD-1 females (Charles River Strain #022). The deletion event was confirmed using PCR primers that flank the predicted deletion (Supplemental Table 1). Germline founders were then backcrossed to C57BL/6 for at least 6 generations to eliminate off-target mutations, and subsequent progeny were used to establish the GPR39-null line. Mice were genotyped using ear biopsies using RT-PCR with specific probes designed for each gene (Transnetyx, Cordova, TN, USA; Supplemental Table 1). Western blot and RT-PCR analysis demonstrated missing GPR39 product in KO mice (Fig. 1). Homozygous GPR39 KO mice are viable, fertile, normal in size, and do not display any overt physical or behavioral abnormalities.

Animals

Male and female GPR39 KO and WT littermates were housed in temperature-controlled rooms on a 12-hour light and 12-hour dark cycle with water and food ad libitum. Animals were randomized to experimental groups, and investigators were blinded to group assignment until datasets were complete and analyzed. All animal procedures were conducted in accordance with National Institute of Health guidelines for use of animals in research, and protocols were approved by the Animal Care and Use Committee at Oregon Health & Science University.

Middle cerebral artery occlusion (MCAO)

Transient focal cerebral ischemia was induced in male (25–32 g) and female (20–25 g) mice at the age of 12–16 weeks using the intraluminal MCAO technique, as previously described. Briefly, isoflurane-anesthetized mice were subjected to 60-min MCAO using a silicone-coated 6 – 0 monofilament (Doccol Corporation, Sharon, MA, USA). The filament was inserted through the right external carotid artery and advanced into the internal carotid artery until laser-Doppler signal dropped to less than 30% of baseline. Mice were kept anesthetized throughout MCAO with % isoflurane and kept warm with water pads and heat lamp. A small laser-Doppler metal probe (Model DRT4, Moor Instruments Inc., Wilmington, DE, USA) was used to monitor cortical perfusion and verify occlusion and reperfusion. After 60 minutes, the filament was withdrawn to allow for reperfusion. Mice were allowed to recover from anesthesia and were subsequently housed in individual cages with free access to food and water until the end of the study. Mice were given daily 0.3 mL intraperitoneal injections of normal saline until they resumed eating solid food (usually within first 3 days). Physiological variables were measured in separate groups of WT and GPR39 KO mice (n = 5 each). Arterial blood pressure was measured continuously throughout MCAO procedure via a femoral arterial catheter. Arterial blood (150 µL) was collected via a femoral artery catheter immediately before and 15 min after MCAO for blood gas measurements using the iSTAT Chem 8 + cartridge (Abbott Point of Care, Princeton, NJ, USA).

Cranial window

Cranial window creation was adapted from in-vivo multiphoton imaging studies.[18] In brief, the cranial window was performed under isoflurane anesthesia (1.0%-1.5%) using a custom-built stereotaxic apparatus to secure the mouse head. A 5-mm-diameter circular craniotomy 1 mm posterior and 3 mm

lateral to bregma was created (Supplemental Fig. 1), closed with 5 mm cover glass (#0 small round cover glass, 5 mm small round, model no. CS-5R-0, Warner Instruments, Holliston, MA, USA), and a custom-built aluminum fixation headplate cemented into place.

Optical Microangiography (OMAG)

OMAG imaging was performed in WT and GPR39 KO mice (n = 10 and 11, respectively) using a previously described system.[17] The animal was immobilized on a custom-made stereotaxic stage and was lightly anesthetized with isoflurane (0.2 L/min O2, 0.8 L/min air). Body temperature was monitored by a rectal thermal probe throughout the experiment, and kept at 36.5 ± 0.5°C by hot water pad and warming blanket. The parietal cranial window was positioned under the OMAG scanning probe and tilted so that it was perpendicular to the light beam with a 10x objective lens. A large field-of-view (FOV) OMAG scan (x-y-z dimensions 2.4 mm x 2.4 mm x 2mm) was taken to ensure landmark positioning, then a smaller OMAG FOV scan (x-y-z 0.5 mm x 0.5 mm x 0.4 mm) was taken at the center for RBC flux measurements. The z dimension (0.4 mm), which represent depth below the cortical surface, was divided into 4 equal layers (100 μm each). OMAG imaging was then performed to assess the total number of RBCs passing through the imaging voxel cross-section per unit time in order to determine RBC flux (Supplemental Fig S1). After removing projection artefact in the scanned volume dataset, the maximum projected en-face image was analyzed separately for each layer to determine average flux within each layer. Flux images were processed to separate dynamic pixels (moving red blood cells within vessels) from static pixels (structural tissue such as vessel walls). Only capillaries were assessed for flux changes using a size filter, excluding all vessels > 10 μm in diameter. At the end of the 24-hour scan, animals were sacrificed and infarct size was measured in these brains as described below. Separate animals were also used for infarct size measurement that did not go through OMAG scanning.

Measurement of infarct size

Mice were euthanized and brains collected and stained with 2,3,5-triphenyltetrazolium chloride (TTC; Sigma, St. Louis, MO, USA) at 24 hours after MCAO.[16] Brain was sectioned into 2-mm thick coronal sections, incubated in TTC, fixed in formalin and digitally analyzed to obtain infarct volume. Infarcted and uninfarcted areas were measured with ImageJ (National Institute of Health, Bethesda, MD, USA). To account for edema, infarct size in each region (cortex, caudate-putamen (CP; striatum) and total hemisphere) was measured as the difference between the contralateral tissue volume and the ipsilateral uninfarcted tissue. Infarct size was measured in male and female WT (n = 9 each) and GPR39 KO (n = 14 and 12, respectively) mice.

Measurement of brain atrophy

For mice surviving 21 days after MCAO, brain damage was evaluated by measuring tissue atrophy rather than infarct because of liquefaction, clearing and scarring after stroke eliminates infarcted tissue. Brains were harvested after behavioral testing in post-operative week 3 (POW3), and cut into 2-mm thick coronal brain sections. Slices were photographed, and the remaining size of each ipsilateral region and its

contralateral counterpart were quantified using ImageJ. The ipsilateral region volume was divided by contralateral volume to determine the percentage volume remaining and atrophied.

Behavior testing after MCAO

Locomotor function (“PRE”) was assessed 24 hours before MCAO surgery (day − 1), and locomotor deficit was evaluated in post-operative week 1 (POW1) and 3 (POW3) using the Cylinder and Pole tests. Details of testing are provided in Supplemental Material. After testing, animals were sacrificed and brains collected to measure brain atrophy, as described above.

Statistical Analysis

Sample sizes were chosen for adequate statistical power (0.8) based on results of prior data sets. Data are presented as mean ± SEM. Analysis was performed using the PRISM 8.0 software. Differences among groups in infarct size, locomotor deficit, atrophy, microvascular perfusion and physiological variables were evaluated by two-way ANOVA with Sidak’s multiple comparisons post hoc test. Separate t-test and ANOVA were performed to assess differences in flux in the deepest cortical layer and overall flux among 4 layers, respectively. Survival and success rates were compared using Gehan-Breslow-Wilcoxon test. Statistical significance was set at $p < 0.05$.

Results

GPR39 deletion increases infarct size after MCAO in male mice

We used a dual guide RNA (gRNA)/CRISPR strategy to generate a GPR39 KO mouse model with a targeted 1322-bp deletion that encompasses exon 1 (Fig. 1A). Loss of GPR39 gene product is documented by RT-PCR (Fig. 1B) and Western blot analysis (Fig. 1C). Figure 2 shows the effect of GPR39 knockout on laser-Doppler perfusion (LDP) and infarct size in male and female GPR3 KO and WT controls. LDP over the MCAO territory was significantly reduced by MCAO, and returned to baseline upon reperfusion, with no difference among groups at any time before, during or after MCAO (Fig. 2A). Despite a similar ischemic insult, male GPR39 KO mice sustained larger infarcts than WT counterparts (55% larger in cortex, 71% in caudate-putamen and 64% in whole hemisphere, Fig. 2B, all $p < 0.03$). In contrast, brain infarct size in female KO mice did not differ from WT female controls in any brain region (Fig. 2C). To further investigate male-specific vulnerability of GPR39 KO to MCAO, male mice were studied further by evaluating the effect of GPR39 knockout on capillary flux in deep brain tissue and on long-term behavioral outcome.

GPR39 KO decreases capillary flux after MCAO in deep cortical layers in male mice

OMAG was employed to assess RBC flux through capillary beds below the cortical surface within the MCA watershed area (penumbra; area highlighted in Fig. 3A and Supplemental Fig. 1). Concomitant with

the larger cortical and CP infarcts in male mice, there was progressive microcirculatory hypoperfusion in the KO group, which was especially evident in deeper layers 3 and 4 (Fig. 3B, $p < 0.03$). Compared to WT controls, post-ischemic RBC flux in layer 3 was halved in the KO group and decreased by 96% in the deepest layer (layer 4, Fig. 3C, $p < 0.05$). This observation is consistent with the dependence of deeper brain tissue on the microcirculation for effective perfusion.

GPR39 KO exacerbates locomotor deficit at 1 week after MCAO

To determine whether increased ischemic damage in GPR39 KO mice affected neurological function, we assessed locomotor behavior at 1 and 3 weeks after MCAO using the Pole and Cylinder tests, and evaluated survival and ipsilateral brain tissue atrophy at these time points (Fig. 4). In the first 7 days after MCAO, GPR39 KO mice died at a higher rate than WT controls (29% vs. 19%, respectively, $p < 0.04$), but mice in both groups who survived to 7 days also survived for the full 21-day study period (Fig. 4A). Using atrophy to index brain injury in mice surviving the full 3 weeks, GPR39 KO mice experienced more atrophy than WT controls in caudate/putamen (by 18%) and whole hemisphere (by 30%; both $p < 0.02$), but not in cortex (Fig. 4B). GPR39 KO mice suffered greater disability than WT controls in both the Cylinder and Pole tests at postoperative week 1 (POW1). In the Cylinder test (Fig. 4C), GPR39 KO mice favored their unaffected paw (positive asymmetry index, where more positivity is worse) than WT controls in POW1, consistent with greater disability. The exaggerated disability was transient, however, disappearing in POW3. Similarly, in the pole test (Fig. 4D), GPR39 KO mice took longer to complete the task than controls at POW1, a deficit also not sustained at POW3.

Hemodynamic and hematological parameters during MCAO

The impact of GPR39 deletion on the hemodynamic and hematological parameters during MCAO was evaluated in separate cohorts of non-surviving mice. As shown in Supplemental Fig S2, no differences were observed between WT and KO mice in arterial blood gases (ABG), base excess, pH, hematocrit and glycemic status before or after MCAO. GPR39 KO mice exhibited a mild hyperkalemic response to MCAO, although baseline kalemia did not differ from WT controls. As in Fig. 2A, no difference in laser-Doppler perfusion over the MCA territory was observed between WT and KO mice at any time (Fig. 5A). Interestingly, we observed an exaggerated drop in blood pressure to blood withdrawals in GPR39 KO mice compared to WT controls (Fig. 5B).

Discussion

Our study reveals several new findings: 1) Targeted deletion of the GPR39 worsens ischemic damage in a sex-specific manner, especially in deeper brain regions in male; 2) Larger infarct in GPR39 KO male mice is associated with impaired capillary reperfusion at 24 hours after stroke, particularly in deeper cortical layers; 3) GPR39 KO male mice sustain larger locomotor deficit 1 week after stroke than WT male mice; 4) GPR39 KO mice experience increased mortality in the first week after focal cerebral ischemia; and 5) GPR39 KO animals are less able to maintain blood pressure under anesthesia during blood withdrawals.

We conclude that the GPR39 gene deletion decreases microvascular reperfusion, exacerbates ischemic brain injury and impairs functional recovery after MCAO. GPR39 may also play a role in preserving systemic blood pressure during blood loss. Taken together, our findings are consistent with a role of GPR39 in control of the microcirculation, such that loss of GPR39 impairs the brain's microvascular capillary response to ischemia and the body's systemic response to hypotension. Thus, preservation or enhancement of GPR39 function during ischemic stroke and systemic hypotension may be protective.

Sex differences in stroke outcomes are well established. The present study extends previous reports by demonstrating a male-specific increase in vulnerability to focal cerebral ischemia as a result of GPR39 KO. The increase in ischemic damage in males is likely linked to poor microvascular perfusion after stroke, as male KO mice had significantly lower capillary flux in deep cortical layers than corresponding WT mice. Poor capillary perfusion in deep cortical layers coincided with the observation that the largest and most consistent regional damage in our study, assessed by measuring either infarct or atrophy, occurred in the deep caudate/putamen (striatum) region. Coexistence of poor microvascular perfusion and larger ischemic damage in the striatum fits the concept that deep brain structures are highly dependent on microvascular flow and are prone to lacunar infarcts due to lack of collaterals connecting penetrating end-arterioles. Moreover, at progressively deeper subcortical layers, capillary RBC flux slows and oxygen extraction increases and becomes more homogenous, again leading to higher dependence of deeper brain tissue on microvascular blood flow.

It is important to note that the failure of capillaries to reperfuse deep brain tissue is observed in mice that had complete restoration of laser-Doppler blood flow on the surface of the brain. This is reminiscent of the clinical observation of incomplete tissue perfusion despite complete large-vessel recanalization after endovascular therapy or t-PA. Our data suggest that GPR39 is an endogenous microvascular protective mechanism, and that enhancing GPR39 activity may protect against microvascular dysfunction after stroke and may serve as a complementary approach to enhance efficacy of endovascular therapy or t-PA.

Our experimental approach allowed us to observe the effect of GPR39 KO on the evolution of infarction over time; from early reperfusion (20 min, in mice used for physiological monitoring), to 24 hours (TTC) and 21 days post-reperfusion (in animals used to measure atrophy). Longitudinal examination shows that maximum CP/striatum damage occurs acutely in GPR39 KO mice, consistent with the role of microcirculation in the acute phase of ischemic injury; whereas more generalized hemispheric damage continues to evolve over time, in part due to secondary inflammation and neurodegeneration. In WT mice, both CP/striatum and generalized hemispheric damage tend to increase more slowly over time, presumably due to intact microvascular protective mechanisms.

In addition to its role in the microcirculation, several, possibly interdependent molecular mechanisms have been proposed by which GPR39 may protect against stroke. First, GPR39 has been shown to reduce excitation of hippocampal neurons by increasing KCC2 expression and chloride efflux and by increasing synthesis of the endocannabinoid 2-arachidonoylglycerol in postsynaptic hippocampal neurons, which moderates presynaptic glutamate release. Furthermore, GPR39 has been proposed to act as a receptor for

zinc, which is released during brain ischemia and has been proposed to play protective and neurotoxic roles.[7] It is possible that receptor activation by zinc could moderate ischemic brain damage. GPR39 has constitutive activity through the Gα/serum responsive element (SRE) cascade, which decreases oxidative, endoplasmic reticulum and mitochondrial stress in hippocampal cell lines, potentially limiting evolving infarct size in penumbral tissues. In addition to neurons, GPR39 is expressed in microglia and peri-capillary cells affected by vascular cognitive impairment.[8] GPR39 may limit inflammation and augment capillary blood flow; thus limiting secondary expansion of infarct during reperfusion. Finally, GPR39 has been proposed to sense the ratio of the vasodilator and protective eicosanoid 14,15-epoxyeicosatrienoate (14,15-EET) to the vasoconstrictor and pro-inflammatory eicosanoid 15-hydroxyeicosatetraeonate (15-HETE).[10] It is possible that increased ischemic injury in GPR39 KO mice is linked to altered interplay between the two eicosanoids. If protective EETs signaling dominates in the setting of ischemia-reperfusion, then loss of GPR39 would be expected to increase injury. On the other hand, if HETEs signaling dominates during blood loss to maintain systemic blood pressure, then loss of GPR39 may explain the exaggerated drop in blood pressure upon blood withdrawal in GPR39 KO mice.

Our results are in agreement with the study by Xie S. et al., which found that a GPR39 *agonist* reduced the infarct size, improved neurological deficit and attenuated neuroinflammation in neonatal hypoxia-ischemia, suggesting that GPR39 plays a protective role in ischemic brain injury. However, another study reported that a GPR39 *antagonist* reduced infarct size and improved tissue perfusion in a mouse model of myocardial ischemia, suggesting that GPR39 plays a detrimental role in ischemic injury in the heart. The discrepancy may be related to lack of specificity of the pharmacological compounds used in these studies to GPR39 when administered in vivo, or to tissue-specific roles of GPR39 in heart vs. brain.

In summary, GPR39 appears to play a beneficial role in recovery from ischemic stroke, and contributes through several pathways that could interact to preserve brain viability and function after stroke. Future studies are required to elucidate if and how pharmacologic activation of GPR39 can decrease infarct size and improve functional outcome after stroke.

Declarations

Ethical Approval and Consent to participate

Not applicable. No human subjects were involved.

Human and Animal Ethics

No studies were performed on human subjects. Studies on animals were conducted in accordance with National Institute of Health guidelines for use of animals in research, and protocols were approved by the Animal Care and Use Committee at Oregon Health & Science University.

Consent for publication

All authors have reviewed the final manuscript, agreed with the content and gave explicit consent to publish it.

Availability of supporting data

The datasets generated during and/or analyzed during the current study are available from the corresponding author on reasonable request.

Competing interests

Dr. Alkayed is co-inventor of technology related to GPR39 that has been licensed to Vasocardea. This potential conflict of interest has been reviewed and managed by Oregon Health and Science University. All other authors have nothing to disclose.

Funding

Supported by NIH grant NS108501 to NJA and Foundation of Anesthesia Education and Research (FAER) grant RFG-08-15-2019 to YX.

Authors' contributions

N.J.A. and Y.X. designed the studies. Y.X., W.H.Z., E.M.A., Z.Y.Q. and T.M.B. performed the studies. Y.X., W.H.Z., E.M.A., Z.Y.Q., T.M.B., Y.L. and R.K.W. analyzed the data and prepared the figures. L.M.F. and A.P.B. designed ad generated the GPR39 knockout mouse. All authors reviewed and approved the manuscript.

Acknowledgements

Not applicable

Authors' information

Yifan Xu, MD, PhD[1]; Wenri H. Zhang, MD, PhD[1]; Elyse M. Allen, BS[1]; Lev M. Fedorov[3], PhD; Anthony P. Barnes, PhD[2], Zu Yuan Qian, PhD[1]; Thierno Madjou Bah, PhD[1]; Yuandong Li, PhD[4]; Ruikang K. Wang, PhD[4], Robert E. Shangraw, MD, PhD[1]; and Nabil J. Alkayed, MD, PhD[1,2]

[1]Departments of Anesthesiology & Perioperative Medicine; [2]Knight Cardiovascular Institute, and [3]Transgenic Mouse Models Shared Resource, Oregon Health & Science University, Portland, OR 97239; [4]Department of Bioengineering, University of Washington School of Medicine, Seattle, WA, USA

References

1. Virani SS et al. Heart Disease and Stroke Statistics-2020 Update: A Report From the American Heart Association. Circulation. 2020;141:e139-e596.

2. Rochmah TN, Rahmawati IT, Dahlui M, Budiarto W, Bilqis N. Economic Burden of Stroke Disease: A Systematic Review. Int J Environ Res Public Health. 2021;18:7552.
3. Evans MRB, White P, Cowley P, Werring DJ. Revolution in acute ischaemic stroke care: a practical guide to mechanical thrombectomy. Pract Neurol. 2017;17:252-265.
4. Goyal M, Menon BK, van Zwam WH, et al. Endovascular thrombectomy after large-vessel ischaemic stroke: a meta-analysis of individual patient data from five randomised trials. Lancet. 2016;387:1723-31.
5. Kloner RA, King KS, Harrington MG. No-reflow phenomenon in the heart and brain. Am J Physiol Heart Circ Physiol. 2018;315:H550-H562.
6. Shabir O, Berwick J, Francis SE. Neurovascular dysfunction in vascular dementia, Alzheimer's and atherosclerosis. BMC Neurosci. 2018;19:62.
7. Xu Y, Barnes AP, Alkayed NJ. Role of GPR39 in Neurovascular Homeostasis and Disease. *Int J Mol Sci*. 2021;22:8200.
8. Davis CM, Bah TM, Zhang WH, et al. GPR39 localization in the aging human brain and correlation of expression and polymorphism with vascular cognitive impairment. Alzheimers Dement (N Y). 2021;7:e12214.
9. Xu Y, Wang M, Xie Y, et al. Activation of GPR39 with the agonist TC-G 1008 ameliorates ox-LDL-induced attachment of monocytes to endothelial cells. Eur J Pharmacol. 2019;858:172451.
10. Alkayed NJ, Cao Z, Qian ZY, et al. Control of coronary vascular resistance by eicosanoids via a novel GPCR. Am J Physiol Cell Physiol. 2022;322:C1011-C1021.
11. Zhang W, Davis CM, Zeppenfeld DM, et al. Role of endothelium-pericyte signaling in capillary blood flow response to neuronal activity. J Cereb Blood Flow Metab. 2021;41:1873-1885.
12. Chorin E, Vinograd O, Fleidervish I, et al. Upregulation of KCC2 activity by zinc-mediated neurotransmission via the mZnR/GPR39 receptor. J Neurosci. 2011;31:12916-26.
13. [1] Besser L, Chorin E, Sekler I, et al. Synaptically released zinc triggers metabotropic signaling via a zinc-sensing receptor in the hippocampus. *J Neurosci*. 2009;29:2890-2901.
14. Doudna JA, Charpentier E. Genome editing. The new frontier of genome engineering with CRISPR-Cas9. Science. 2014;346:1258096.
15. Qin W, Kutny PM, Maser RS, et al. Generating Mouse Models Using CRISPR-Cas9-Mediated Genome Editing. Curr Protoc Mouse Biol. 2016;6:39-66.
16. Zhang W, Koerner IP, Noppens R, Grafe M, Tsai HJ, Morisseau C, Luria A, Hammock BD, Falck JR, Alkayed NJ. Soluble epoxide hydrolase: a novel therapeutic target in stroke. J Cereb Blood Flow Metab. 2007;27:1931-40.
17. Baran U, Zhu W, Choi WJ, et al. Automated segmentation and enhancement of optical coherence tomography-acquired images of rodent brain. J Neurosci Methods. 2016;270:132-137.
18. Zhang W, Davis CM, Zeppenfeld DM, Golgotiu K, Wang MX, Haveliwala M, Hong D, Li Y, Wang RK, Iliff JJ, Alkayed NJ. Role of endothelium-pericyte signaling in capillary blood flow response to neuronal

activity. J Cereb Blood Flow Metab. 2021 Aug;41(8):1873-1885.
19. Li Y, Choi WJ, Wei W, et al. Aging-associated changes in cerebral vasculature and blood flow as determined by quantitative optical coherence tomography angiography. Neurobiol Aging. 2018;70:148-159.
20. Brait VH, Wright DK, Nategh M, et al. Longitudinal hippocampal volumetric changes in mice following brain infarction. Sci Rep. 2021;11:10269.
21. Balkaya M, Kröber JM, Rex A, Endres M. Assessing post-stroke behavior in mouse models of focal ischemia. J Cereb Blood Flow Metab. 2013;33:330-8.
22. Alkayed NJ, Harukuni I, Kimes AS, London ED, Traystman RJ, Hurn PD. Gender-linked brain injury in experimental stroke. Stroke. 1998;29:159-65.
23. Feekes JA, Cassell MD. The vascular supply of the functional compartments of the human striatum. Brain. 2006;129(Pt 8):2189-201.
24. Li B, Esipova TV, Sencan I, Kılıç K, et al. More homogeneous capillary flow and oxygenation in deeper cortical layers correlate with increased oxygen extraction. Elife. 2019;8:e42299.
25. Gilad D, Shorer S, Ketzef M, et al. Homeostatic regulation of KCC2 activity by the zinc receptor mZnR/GPR39 during seizures. Neurobiol Dis. 2015;81:4-13.
26. Perez-Rosello T, Anderson CT, Schopfer FJ, et al. Synaptic Zn2+ inhibits neurotransmitter release by promoting endocannabinoid synthesis. J Neurosci. 2013;33:9259-72.
27. Koh JY, Suh SW, Gwag BJ, He YY, Hsu CY, Choi DW. The role of zinc in selective neuronal death after transient global cerebral ischemia. Science. 1996;272:1013-6.
28. Galasso SL, Dyck RH. The role of zinc in cerebral ischemia. Mol Med. 2007;13:380-7.
29. Dittmer S, Sahin M, Pantlen A, et al. The constitutively active orphan G-protein-coupled receptor GPR39 protects from cell death by increasing secretion of pigment epithelium-derived growth factor. J Biol Chem. 2008;283:7074-81.
30. Xie S, Jiang X, Doycheva DM,et al. Activation of GPR39 with TC-G 1008 attenuates neuroinflammation via SIRT1/PGC-1α/Nrf2 pathway post-neonatal hypoxic-ischemic injury in rats. J Neuroinflammation. 2021;18:226.
31. Methner C, Cao Z, Mishra A, Kaul S. Mechanism and potential treatment of the "no reflow" phenomenon after acute myocardial infarction: role of pericytes and GPR39. Am J Physiol Heart Circ Physiol. 2021;321:H1030-H1041.

Figures

Figure 1

Creation and confirmation of mouse GPR39 knockout model. A. Schematic of mouse GPR39 gene locus targeting strategy. Guide RNAs were designed to cleave at sites flanking exon 1 of Gpr39 resulting in a 1322 base pair deletion. Exon 2 was left intact. **B.** RT-PCR and **C**. Western blot of GPR39 (top row) and beta-Actin (bottom row) confirming presence of GPR39 mRNA (**B**) and protein (**C**) in brain, heart and kidneys from wild type mice (left) but absent in GPR39 knockout mice (right).

Figure 2

GPR39 deletion increases infarct size in male mice after MCAO. A. Relative laser Doppler perfusion of MCA territory. There were no differences among groups. **B.** Infarct size was significantly larger in male GPR39 KO mice compared to WT littermates in cerebral cortex, caudate putamen (CP) and whole hemisphere. **C.** There was no difference in infarct size between WT and GPR39 KO in females. GPR39 KO vs. WT. n.s., not significant. **p<0.05, ** p<0.001*.

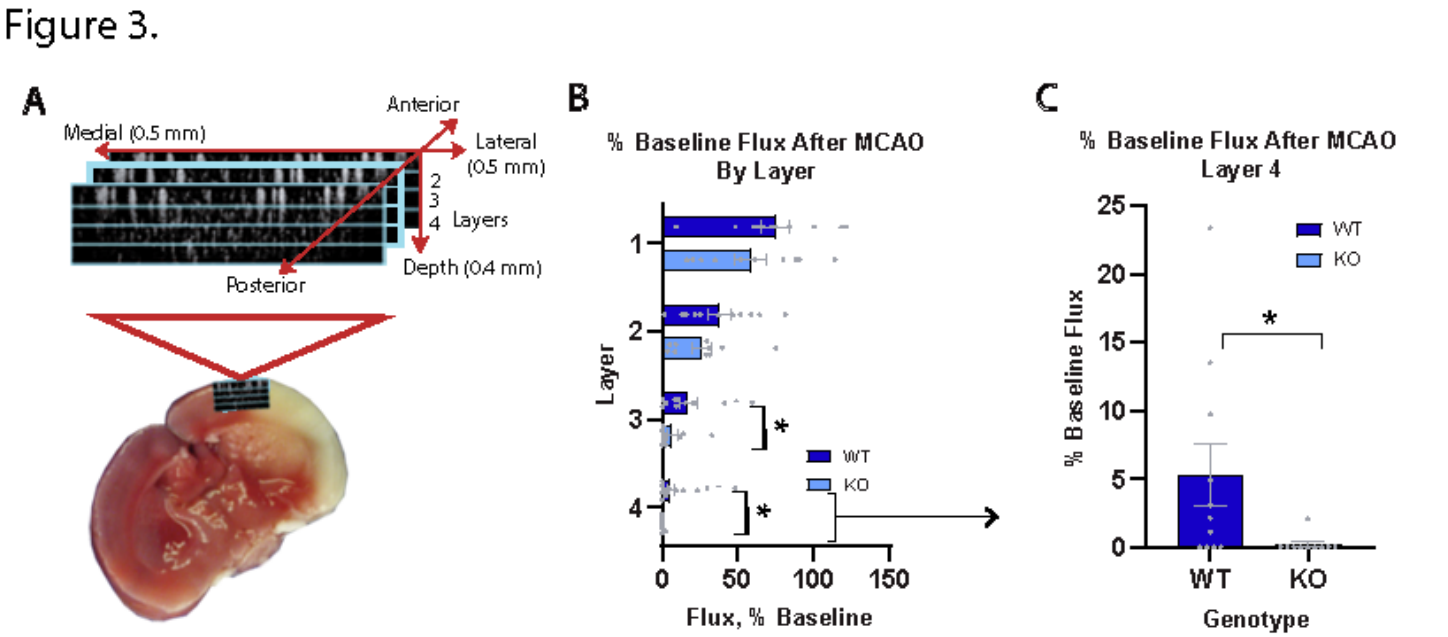

Figure 3

Optical microangiography (OMAG) demonstrates worsened microvascular brain tissue perfusion in GPR39 KO vs WT males after stroke. **A**. Schematic of OMAG setup for capillary blood flow measurement in 4 cortical layers within ischemic penumbra. **B.** Post-stroke cortical capillary flux in in layers 1-4 (% baseline) in GPR39 KO and WT littermates. (Genotype $F_{1,76}$ = 5.36; **p*<0.0234*)*. **C**. Post-stroke capillary flux in GPR39 KO vs. WT littermates in deepest cortical layer only (#4). (n=10 KO, n=11 WT, **p<0.05*).

Figure 4

GPR39 KO decreases survival and motor function 1 week after stroke, and increases brain atrophy 3 weeks after stroke. A. Timeline of behavior testing, MCAO, infarct size and brain atrophy measurement, superimposed on survival curve. GPR39 KO decreased survival at 1 week compared to WT (*$p<0.05$). **B.** Ipsilateral atrophy in cortex, caudate putamen (CP) and hemisphere in KO and WT mice at 3 weeks after stroke. **C.** KO mice show greater forepaw disability in the Cylinder test 1 week after stroke. Higher asymmetry indicates greater disability. **D.** KO mice show decreased coordination in the Pole test 1 week after stroke. Longer time indicates greater disability. Total number of KO and WT mice at beginning of protocol was 24 and 21, respectively. Number of mice at full survival to 21 days was 17 in each group (*$P<0.05$).

Figure 5

Hemodynamic measures in GPR39 KO and WT mice during and after stroke. A. Relative laser-Doppler perfusion over the MCA territory during and 15 min after MCAO, n.s. not significant. **B**. Mean arterial pressure (MAP), as % baseline, in cohort used for arterial blood gas measurement. (Genotype $F_{1,32}$ = 10.05; **p<0.0034; post final ABG adjusted p value for multiple comparisons *$p<0.05$).

Supplementary Files

This is a list of supplementary files associated with this preprint. Click to download.

- SupplementalMaterial.docx